US008209083B2

(12) United States Patent
Ganguli et al.

(10) **Patent No.: US 8,209,083 B2**
(45) **Date of Patent: Jun. 26, 2012**

(54) **TUNABLE ARCHITECTURE FOR AIRCRAFT FAULT DETECTION**

(75) Inventors: **Subhabrata Ganguli**, Plymouth, MN (US); **George Papageorgiou**, Minneapolis, MN (US); **Sonja Glavaski-Radovanovic**, Plymouth, MN (US)

(73) Assignee: **Honeywell International Inc.**, Morristown, NJ (US)

(*) Notice: Subject to any disclaimer, the term of this patent is extended or adjusted under 35 U.S.C. 154(b) by 1287 days.

(21) Appl. No.: **11/462,481**

(22) Filed: **Aug. 4, 2006**

(65) **Prior Publication Data**

US 2010/0241293 A1 Sep. 23, 2010

(51) **Int. Cl.**
G01M 17/00 (2006.01)

(52) **U.S. Cl.** **701/34.1**; 701/3; 701/32.9; 706/20; 706/913

(58) **Field of Classification Search** .... 701/3, 4, 701/8, 10, 11, 12, 14, 29, 31, 34, 35; 244/76 R, 244/194, 195; 706/12, 20, 25, 45–47, 913
See application file for complete search history.

(56) **References Cited**

U.S. PATENT DOCUMENTS

6,298,286	B1	10/2001	Ying	
6,622,134	B1 *	9/2003	Sorkin	706/20
2003/0074159	A1 *	4/2003	Bechhoefer et al.	702/181
2005/0228783	A1 *	10/2005	Shanahan et al.	707/3

FOREIGN PATENT DOCUMENTS

DE	4022954	1/1992
EP	1122694	8/2001
WO	9800334	1/1998

OTHER PUBLICATIONS

Glavaski et al, Reconfigurable Control for Active Management of Aircraft System Failures, Jun. 2001, Procedings of the American Control Conference.*

Schneider et al, Fuzzy Logic Baased Threshold Adaption for Fault Detection in Robots, 1994, University of Duisburg.*

Sanjay, Guidance, Navigation and Control Center of Excellence, Mar. 2, 2005, Honeywell, slide 6.*

Astrom et al., “Estimator Implementation”, “Adaptive Control”, 1995, pp. 465-480, Publisher: Addison Wesley.

Becastro et al., “Application of Failure Detection, Identification, and Accomodation Methods for Improved Aircraft Safety”, “Proceedings of the American Control Conference”, Jun. 2001, pp. 2623-2624, vol. 4, Publisher: ACC, Published in: Evanston, IL.

(Continued)

Primary Examiner — Khoi Tran
Assistant Examiner — Spencer Patton
(74) *Attorney, Agent, or Firm* — Ingrassia, Fisher & Lorenz, P.C.

(57) **ABSTRACT**

A method for detecting faults in an aircraft is disclosed. The method involves predicting at least one state of the aircraft and tuning at least one threshold value to tightly upper bound the size of a mismatch between the at least one predicted state and a corresponding actual state of the non-faulted aircraft. If the mismatch between the at least one predicted state and the corresponding actual state is greater than or equal to the at least one threshold value, the method indicates that at least one fault has been detected.

19 Claims, 3 Drawing Sheets

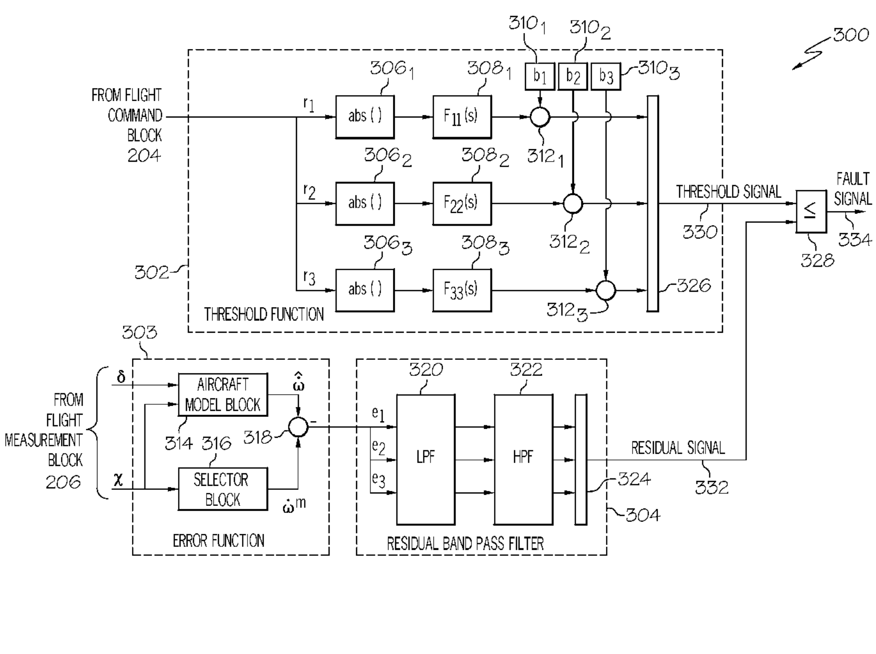

OTHER PUBLICATIONS

Brinker et al., "Reconfigurable Flight Control for a Tailless Advanced Fighter Aircraft", "AIAA Guidance, Navigation, and Control Conference and Exhibit", 1998, pp. 75-87, No. 1, Publisher: AIAA With Permission From the Boeing Company.

Calise et al., "Neural Networks for Feedback Linearization in Aircraft Control", "A Collection of Technical Papers: AIAA Guidance, Navigation, and Control Conference", 1992, pp. 395-406, Publisher: AIAA.

Elgersma et al., "Parameter Identificiation for Systems With Redundant Actuators", "AIAA Guidance, Navigation, and Control Conference and Exhibit, A Collection of Technical Papers", 1998, pp. 109-117, No. 1, Publisher: AIAA.

Ganguli et al., "Piloted Simulation of Fault Detection, Isolation and Reconfiguration Algorithms for a Civil Transport Aircraft", "Proceedings of the AIAA Guidance, Navigation and Control Conference", Aug. 2005, Publisher: AIAA.

Glavaski et al., "Active Failure Management for Aircraft Control Recovery", "Proceedings of the AIAA Guidance, Navigation and Control Conference", Aug. 2002, pp. 1-8, Publisher: AIAA.

Glavaski et al, "Failure Accommodating Aircraft Control", "Proceedings of the American Control Conference", May 2002, Publisher: AACC.

Glavaski et al, "Reconfigurable Control for Active Management of Aircraft System Failures", "Proceedings of the American Control Conference", Jun. 2001, pp. 1-20, Publisher: AACC.

Gunn, "Matlab SVM Toolbox", "Support Vector Machines for Classification and Regression, Technical Report", May 10, 1998, p. 51 Publisher: University of Southampton, Published in: Southampton, UK.

Ha et al., "Generalization Bounds for Weighted Binary Classification With Applications to Statistical Verification", "International Joint Conference on Artificial Intelligence", 2005.

Jorgensen, "Feedback Linearized Aircraft Control Using Dynamic Cell Structures", "Soft Computing, Multimedia and Image Processing, Recent Trends, Principals and Applications", 1998, pp. 207-212, vol. 8, Publisher: TSI Press, Published in: Albuquerque, NM.

Kim et al., "Nonlinear Flight Control Using Neural Networks", "Journal of Guidance, Control, and Dynamics", Sep. 17, 1996, pp. 26-33, vol. 20, No. 1, Publisher: AIAA.

Mercadante, "Piloted Simulation Verification of a Control Reconfiguration Strategy for a Fighter Aircraft Under Impairments", "AGARD Conference Proceedings, Fault Tolerant Design Concepts for Highly Integrated Flight Critical Guidance and Control Systems", Oct. 1989, pp. 51-1-51-24, No. 465, Publisher: NATO Advisory Group for Areospace Research and Development, Published in: Toulouse, France.

Monaco et al., "Implementation and Flight Test Assessment of an Adaptive, Reconfigurable Flight Control System", "AIAA Guidance, Navigation, and Control Conference", Aug. 1997, pp. 1443-1454, No. 3, Publisher: AIAA.

Steinberg, "A Histrocial Overview of Research in Reconfigurable Flight Control", "Journal of Areospace Engineering: Special Issue Paper", Aug. 2005, pp. 263-275, vol. 219, No. G4, Publisher: The Institution of Mechanical Engineers.

Steinberg, "An Initial Assessment of Neural Netwrok and Fuzzy Logic Technology for Flight Control Systems", "Proceedings of the American Control Conference", Jun. 1994, pp. 173-177, vol. 1, Publisher: AACC, Published in: Baltimore, MD.

Totah , "Simulation Evaluation of a Neural-Based Flight Controller", "Proceedings of the AIAA Flight Simulation Technologies Conference, Technical Papers", 1996, pp. 259-266, Publisher: AIAA.

Tucker, "Touchdown, The Development of Propulsion Control Aircraft at NASA Dryden", "Monographs in Aerospace History", 1999, No. 16, Publisher: NASA, Published in: Washington D.C.

Weiss et al., "Integrated Restructurable Flight Control System Demonstration Results", "NASA Contractor Report 178305", May 1987, Publisher: NASA.

Gutierrez-Osuna , "Lecture Notes on Pattern Recognition and Intelligent Sensor Machines (PRISM): Lecture 21: Support Vector Machines", "http://research.cs.tamu.edu/prism/lectures.htm", access on Jun. 9, 2010, Publisher: Texas A & M University.

Ljung, L. and Soderstrom, T. , "Theory and Practice of Recursive Identification, Series in Signal Processing, Optimization, and Control", 1983, pp. 370-403, No. 7, Publisher: MIT Press.

Vapnik, "Statisical Learning Theory", 1998, pp. 401-441, No. 10, Publisher: Wiley.

* cited by examiner

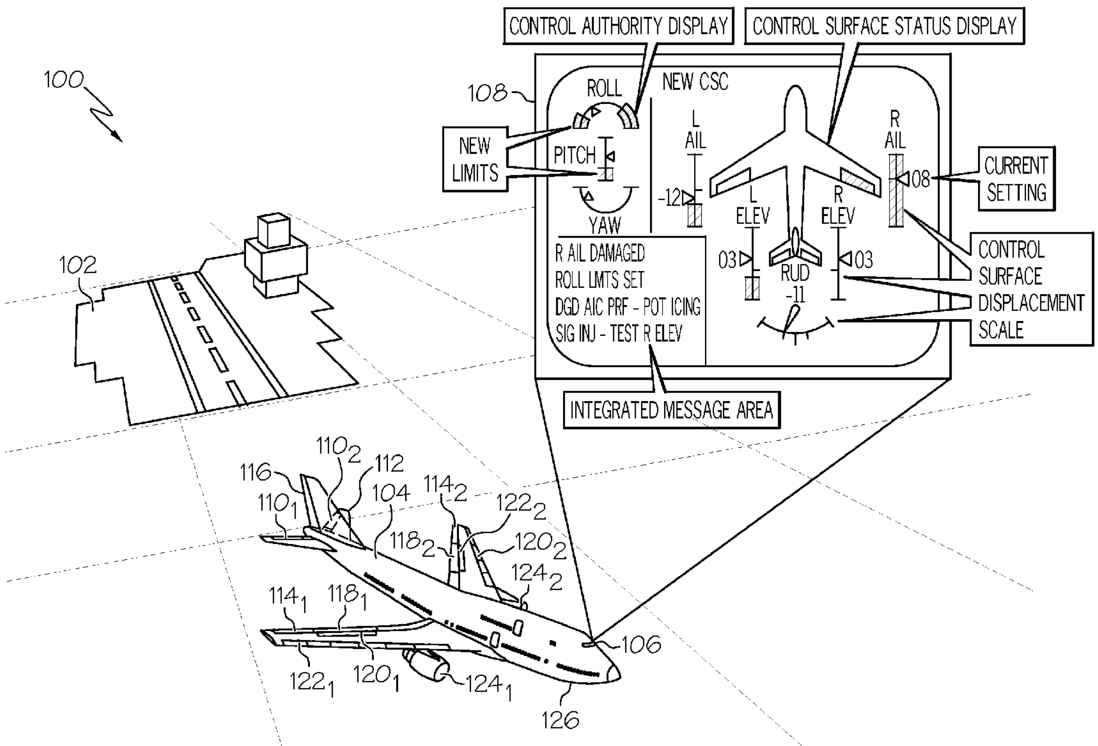
CONTROL AUTHORITY DISPLAY
CONTROL SURFACE STATUS DISPLAY
100
108
ROLL
NEW CSC
NEW LIMITS
PITCH
L AIL
R AIL
CURRENT SETTING
-12
08
YAW
L ELEV
R ELEV
CONTROL SURFACE DISPLACEMENT SCALE
03
03
RUD
-11
R AIL DAMAGED
ROLL LMTS SET
DGD AIC PRF - POT ICING
SIG INU - TEST R ELEV
102
INTEGRATED MESSAGE AREA
116
110_2
112
110_1
104
114_2
122_2
118_2
120_2
124_2
114_1
118_1
106
122_1
120_1
124_1
126

FIG. 1

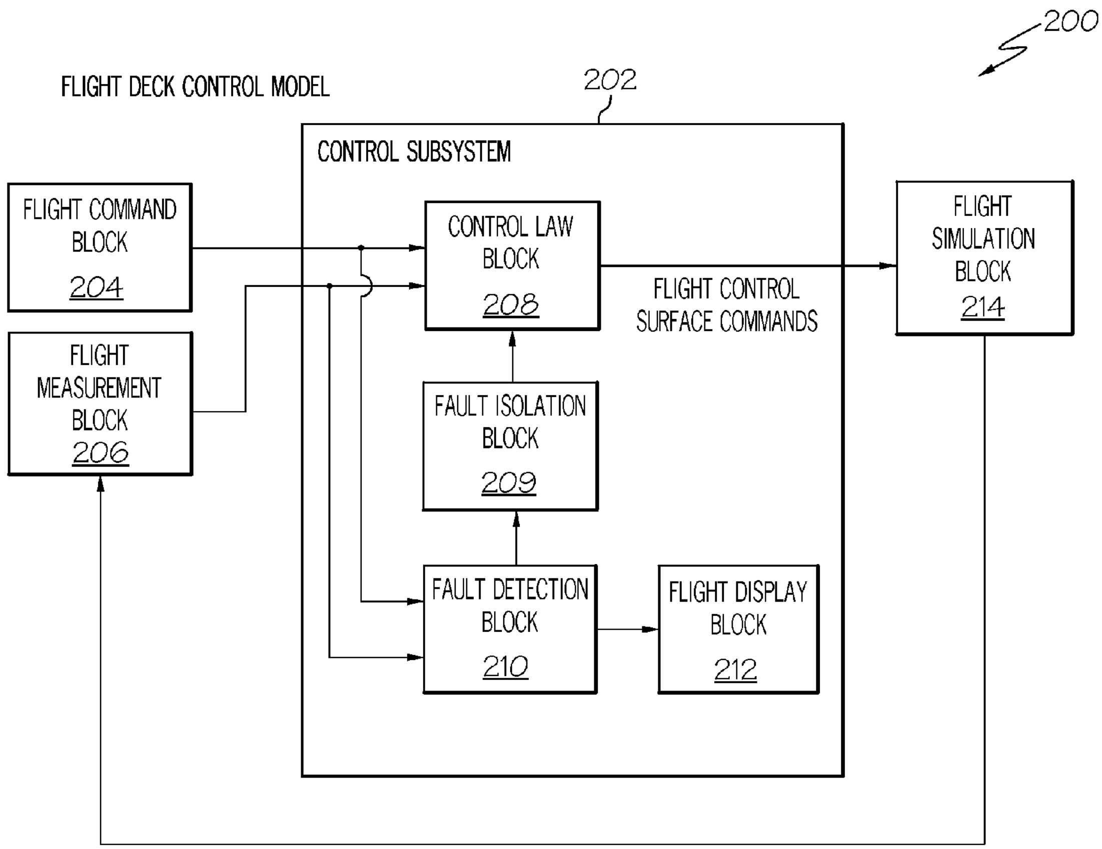
200
FLIGHT DECK CONTROL MODEL
202
CONTROL SUBSYSTEM
FLIGHT COMMAND BLOCK 204
FLIGHT MEASUREMENT BLOCK 206
CONTROL LAW BLOCK 208
FAULT ISOLATION BLOCK 209
FAULT DETECTION BLOCK 210
FLIGHT DISPLAY BLOCK 212
FLIGHT CONTROL SURFACE COMMANDS
FLIGHT SIMULATION BLOCK 214

FIG. 2

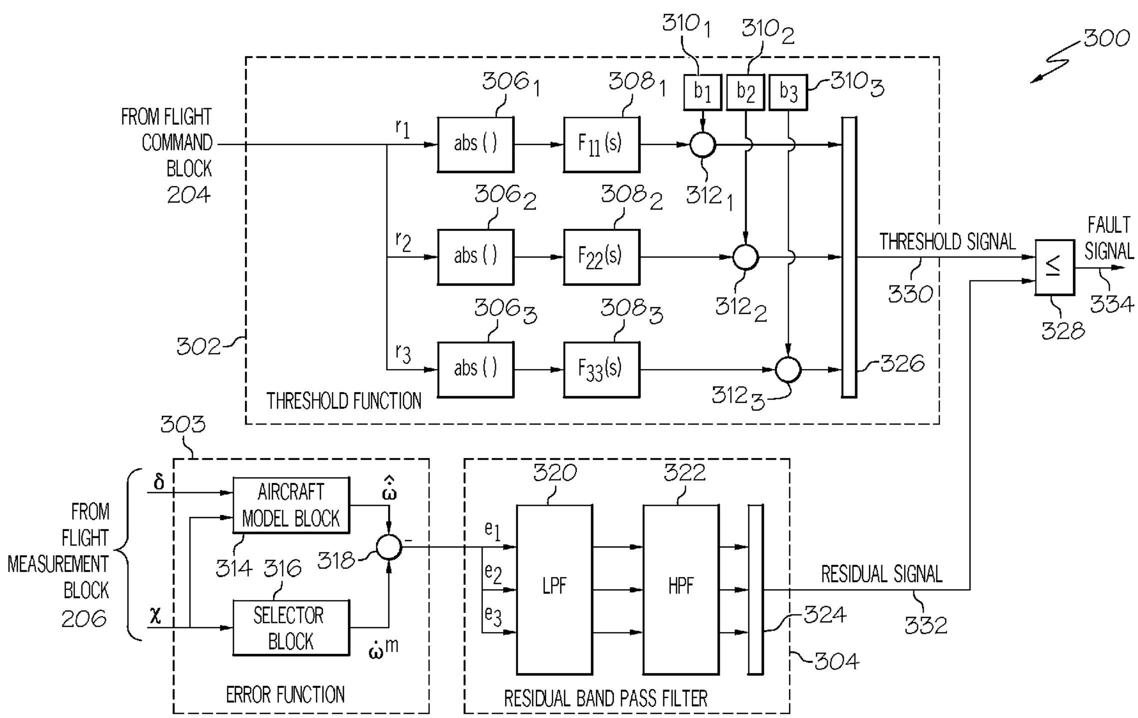

300
FROM FLIGHT COMMAND BLOCK 204
r1
r2
r3
abs ( )
F11(s)
F22(s)
F33(s)
b1
b2
b3
310 1
310 2
310 3
306 1
306 2
306 3
308 1
308 2
308 3
312 1
312 2
312 3
326
302
THRESHOLD FUNCTION
THRESHOLD SIGNAL
330
FAULT SIGNAL
334
328
303
FROM FLIGHT MEASUREMENT BLOCK 206
δ
χ
AIRCRAFT MODEL BLOCK
SELECTOR BLOCK
314 316
318
ERROR FUNCTION
320
322
e1
e2
e3
LPF
HPF
324
304
RESIDUAL BAND PASS FILTER
RESIDUAL SIGNAL
332

FIG. 3

TUNABLE ARCHITECTURE FOR AIRCRAFT FAULT DETECTION

GOVERNMENT INTEREST STATEMENT

The invention described herein was made in the performance of work under NASA Contract No. NAS1-00107 and is subject to the provisions of Section 305 of the National Aeronautics and Space Act of 1958 (42 U.S.C. 2457).

BACKGROUND

Fast and reliable failure detection is crucial for damaged aircraft to maintain controlled flight. The two main objectives of the U.S. Government's Aviation Safety Program are to develop and demonstrate technologies that reduce aircraft accident rates, and develop technologies that reduce aviation injuries and fatalities when accidents do occur. Fault detection, isolation, and reconfiguration (FDIR) for flight control continues to be an active area of research in the aerospace community. To date, a wide variety of technologies have been demonstrated in high-fidelity simulations (that is, simulations with minimal distortions) and in actual flight tests with various levels of success.

For model-based aircraft fault detection, a mathematical model of the aircraft is used. Model-based fault detection is based on comparing measurements from the aircraft with corresponding error predictions from the aircraft model (that is, residual processing). In real life situations, the comparison of these signals is not trivial. This is due to the fact that (typically) there are imperfections in most mathematical flight simulation models coinciding with multiple sources of aircraft measurements errors. Therefore, any fault detection algorithms require fast and reliable processing in the presence of modeling and measurement errors.

SUMMARY

The following specification addresses an architecture and tuning procedure for aircraft fault detection. Particularly, in one embodiment, a method for detecting faults in an aircraft is provided. The method involves predicting at least one state of the aircraft and tuning at least one threshold value to tightly upper bound the size of a mismatch between the at least one predicted state and a corresponding actual state of the non-faulted aircraft. If the mismatch between the at least one predicted state and the corresponding actual state is greater than or equal to the at least one threshold value, the method indicates that at least one fault has been detected.

DRAWINGS

These and other features, aspects, and advantages will become better understood with regard to the following description, appended claims, and accompanying drawings where:

FIG. **1** is an illustration of an embodiment of a flight system;

FIG. **2** is a block diagram of an embodiment of a flight deck control model; and

FIG. **3** is a block diagram of an embodiment of a fault detection module within the flight deck control model of FIG. **2**.

Like reference numbers and designations in the various drawings indicate like elements.

DETAILED DESCRIPTION

FIG. **1** is an illustration of an embodiment of a flight system **100**. The flight system **100** comprises an aircraft **104** and a

flight deck **106**. For the purposes of this description, FIG. **1** includes an airport **102**. The airport **102** is representative of a typical airport with a runway suitable for takeoffs and landings of the aircraft **104**. The flight deck **106** is responsible for activating and monitoring flight controls for the aircraft **104**. The aircraft **104** is shown by way of example and not by way of limitation. In one embodiment, the aircraft **104** is representative of a typical aircraft (for example, a twin-engine transport aircraft, or the like) with longitudinal and lateral/directional axes control surfaces. In the example embodiment of FIG. **1**, the plurality of control surfaces comprise, without limitation, elevators $\mathbf{110}_1$ and $\mathbf{110}_2$ and a stabilizer **112** for longitudinal-axis control of the aircraft **104**. Additional control surfaces of the aircraft **104** include, without limitation, ailerons $\mathbf{114}_1$ and $\mathbf{114}_2$, a rudder **116**, flaps $\mathbf{118}_1$ and $\mathbf{118}_2$, slats $\mathbf{120}_1$ and $\mathbf{120}_2$, and spoilers $\mathbf{122}_1$ and $\mathbf{122}_2$ to provide lateral/directional control of the aircraft **104**. The aircraft **104** further includes, without limitation, engines $\mathbf{124}_1$ and $\mathbf{124}_2$, and landing gear **126**. It is further understood that the arrangement of the plurality of control surfaces on the aircraft **104** as shown in FIG. **1** is one example of an acceptable arrangement, and that other arrangements are possible.

The flight deck **106** further includes a flight display **108**. In the example embodiment of FIG. **1**, the flight display **108** is a version of a flight display for a Control Upset Prevention and Recovery System (CUPRSys), or the like, that simulates aircraft failure prevention and recovery on a plurality of civilian, commercial or military aircraft. In one implementation, the flight display **108** displays, without limitation, angular acceleration of the aircraft **104** and pitch, roll and yaw of the aircraft **104** with respect to a rotating earth. The flight display **108** further indicates, without limitation, effects of current control surface positions (of the plurality of control surfaces discussed above, including the landing gear **126**) on the aerodynamics of the aircraft **104**. Additional aircraft state information provided by the flight display **108** includes, without limitation, performance of engines $\mathbf{124}_1$ and $\mathbf{124}_2$, landing gear **126**, and current atmosphere and turbulence measurements. In the example embodiment of FIG. **1**, any potential aircraft fault of the aircraft **104** are visually displayed in the flight deck **106** by the flight display **108**. In one implementation, potential aircraft faults include, without limitation, stuck and floating flight control surfaces due to a hydraulic or mechanical malfunction, reduced surface effectiveness due to a surface loss, an engine failure, a landing gear failure, and a buildup of ice on one or more flight control surfaces.

A simulated model of the aircraft **104** includes a tunable architecture for aircraft fault detection such as further described, for example, with respect to FIG. **3** below. The tunable architecture for aircraft fault detection will substantially minimize (that is, reduce) the number of false alarms (due to any mismatches in actual aircraft states versus predicted aircraft states of the aircraft **104**) while maintaining a required level of fault detection. The simulated model of the aircraft **104** (discussed below with respect to FIG. **2**) is concerned with detecting faults (that is, equivalent aircraft-to-model mismatches) for proper flight deck control in the flight deck **106** during an actual flight.

FIG. **2** is a block diagram of an embodiment of a flight deck control model **200**. In the example embodiment of FIG. **2**, the flight deck control model **200** is a flight control simulation of the aircraft **104** of FIG. **1**. The flight deck control model **200** further comprises a control subsystem **202**, a flight command block **204**, a flight measurement block **206**, and a flight simulation block **214**. The control subsystem **202** further includes a control law block **208**, a fault isolation block **209**, a fault detection block **210**, and a flight display block **212**. Both the flight command block **204** and the flight measurement block **206** are in communication with the control law block **208** and the fault detection block **210**. The fault isolation block **209** is in communication with the control law block **208**. The fault detection block **210** is in communication with the fault isolation block **209** and the flight display block **212**. The flight display block **212** is representative of the flight display **108** of FIG. **1**.

In one implementation, the flight command block **204** represents flight commands received from an operator (pilot) navigating the aircraft **104** of FIG. **1**. Moreover, the flight simulation block **214** represents the aircraft **104**. The flight simulation block **214** continuously issues one or more simulated control surface position sensor outputs and one or more aircraft state outputs to the flight measurement block **206**. The flight measurement block **206** predicts at least one aircraft state of the flight simulation block **214**. The flight deck control model **200** models operational behavior of the flight simulation block **214** so that any mismatch is reduced in actual movements versus predicted movements of the non-faulted aircraft model block **214**. The flight deck control model **200** reconfigures control of the flight deck **106** in real-time based on a tunable fault detection algorithm and a fault isolation algorithm. The tunable fault detection algorithm is described further below in connection with FIG. **3**. By incorporating the tunable fault detection algorithm, the flight deck control model **200** maintains a required level of fault detection for at least the aircraft faults discussed above with respect to FIG. **1**.

In operation, the control law block **208** and fault detection block **210** receive one or more flight commands from the flight command block **204**. The control law block **208** and fault detection block **210** receive one or more aircraft state measurements from the flight measurement block **206**. The control law block **208** controls one or more positions of the plurality of flight control surfaces discussed above with respect to FIG. **1**. To accomplish this, the control law block **208** receives one or more input commands from the flight command block **204** and the flight measurement block **206**. The one or more input commands include, without limitation, a roll rate (p), a blend of pitch rate and normal acceleration (C*), and an angle-of-sideslip (β). From the one or more input commands received, the control law block **208** issues one or more flight control surface commands to the flight simulation block **214**. The one or more flight control surface commands include, without limitation, an aileron difference between the ailerons $\mathbf{114}_1$ and $\mathbf{114}_2$ of FIG. **1**, an average elevator for the elevators $\mathbf{110}_1$ and $\mathbf{110}_2$ of FIG. **1**, and the rudder **116** of the aircraft **104**. In one implementation, the control law block **208** generates roll, pitch, and yaw commands based on the one or more aircraft state measurements from the flight measurement block **206**. The control law block **208** allocates at least one flight control surface command for every corresponding flight control surface on the aircraft model block **214**.

The fault detection block **210** models non-linear equations of motion of the aircraft **104** through a constant matrix H^M (the control law block **208** uses the same model structure with a different constant matrix H^C). In one implementation, the fault isolation block **209** estimates the change in H^M (ΔH^M) for every fault that the fault detection block **210** detects using a recursive least squares (RLS) estimator. The RLS estimator receives a processed state of the aircraft **104**, one or more control surface position measurements of the aircraft **104**, and one or more angular accelerations of the aircraft **104** from the fault detection block **210**. The fault isolation block **209** isolates at least one fault when the estimate of ΔH^M converges. Once the at least one fault is isolated, the fault isolation block **209** updates the control law block **208** with a reconfigured control law (that is, reconfigures the H^C if matrix). At substantially the same time, the pilot display block **212** notifies the flight display **108** of FIG. **1** with a status and potential impact of the at least one detected fault on the aircraft **104**.

From the aircraft state measurements and the one or more flight control surface position measurements, the flight measurement block **206** predicts (that is, estimates) angular acceleration of the aircraft **104** in all three axes (that is, the x, y and z axes). The fault detection block **210** determines a difference (that is, an error) between measured and estimated angular accelerations to produce a residual signal (as further discussed in detail below with respect to FIG. **3**). The residual signal is subsequently compared to a fault detection threshold within the fault detection block **210**. When the residual signal is greater than the fault detection threshold, a fault is flagged on the flight display block **212**. As further discussed in detail below with respect to FIG. **3**, the fault detection block **210** tightly bounds one or more differences between predicted states and actual states of the non-faulted aircraft **104**. The fault detection block **210** is further responsible for substantially minimizing missed fault detections and reducing false alarms. To substantially minimize and reduce false alarms due to wind gusts, the fault detection threshold within the fault detection block **210** is also made a function of measured linear accelerations.

FIG. **3** is a block diagram of an embodiment of a fault detection module **300** within the flight deck simulation model of FIG. **2**. In the example embodiment of FIG. **3**, the fault detection module **300** is further representative of the fault detection block **210** of FIG. **2** discussed above. The fault detection module **300** comprises a threshold function **302**, an error function **303**, and a residual band pass filter **304**. The threshold function **302** further comprises absolute measurement functions $\mathbf{306}_1$ to $\mathbf{306}_3$, threshold filter functions $\mathbf{308}_1$ to $\mathbf{308}_3$, bias model blocks $\mathbf{310}_1$ to $\mathbf{310}_3$, threshold summation points $\mathbf{312}_1$ to $\mathbf{312}_3$, and a threshold signal multiplexer **326**. The residual band pass filter **304** comprises a low pass filter function **320**, a high pass filter function **322**, and a residual signal multiplexer **324**. The residual signal multiplexer **324** issues a residual signal **332** to a comparator function **328**. The comparator function **328** computes a fault signal **334** as a potential fault detection signal for the flight display block **212** of FIG. **2**.

The threshold function **302** accepts at least three reference commands (indicated as r_1 to r_3 in FIG. **3**) from the flight command block **204** of FIG. **2**. The threshold function **302** transfers each of the at least three reference commands r_1 to r_3 to corresponding absolute measurement functions $\mathbf{306}_1$ to $\mathbf{306}_3$ and threshold filter functions $\mathbf{308}_1$ to $\mathbf{308}_3$ for each axis of motion. Each threshold summation point $\mathbf{312}_1$ to $\mathbf{312}_3$ receives an output from the corresponding threshold filter function $\mathbf{308}_1$ to $\mathbf{308}_3$ and at least one bias value from corresponding bias model blocks $\mathbf{310}_1$ to $\mathbf{310}_3$. Each bias model block **310** compensates (accommodates) for one or more external (unmeasured) disturbances (for example, atmospheric turbulence) on each axis of motion. The threshold signal multiplexer **326** issues a threshold signal **330** to the comparator function **328**.

The error function **303** comprises an aircraft model block **314** and a selector block **316** coupled to a differencer **318**. The aircraft model block **314** receives one or more control surface positions and one or more actual aircraft states from the flight measurement block **206** of FIG. **2**. The selector block **316** receives the one or more actual aircraft states from the flight measurement block **206**. The aircraft model block **314** determines an estimated angular acceleration of the aircraft **104** (indicated as $\hat{\dot{\omega}}$ in FIG. **3**). The selector block **316** derives a measured angular acceleration of the aircraft **104** (indicated as $\dot{\omega}^m$ in FIG. **3**) from the one or more actual aircraft states (indicated as χ in FIG. **3**). As further illustrated below, the differencer **318** differences the estimated angular acceleration and the measured angular acceleration of the aircraft **104** in all three axes of motion to produce error signals e_1 to e_3. The residual band pass filter **304** filters the error signals e_1 to e_3 from the error function **303** to remove control surface trim and measurement errors, creating the residual signal **332**.

Error Processing of Measured vs. Estimated Aircraft States

A model of the one or more aircraft states from the flight measurement block **206** of FIG. **2** is illustrated below in Equation 1.

$$\dot{x}=f(x,u),\ \omega=Cx \Rightarrow \dot{\omega}=Cf(x,u) \qquad \text{(Equation 1)}$$

With respect to Equation 1 above, $x \in R^n$ denotes an actual aircraft state vector, $u \in R^m$ denotes a control surface input vector, and $\omega \in R^3$ denotes an angular velocity vector. In one implementation, C contains zeroes and ones. Measurements of x and u are represented below in Equation 2.

$$x^m=x+\delta x,\ u^m=u+\delta u \qquad \text{(Equation 2)}$$

With respect to Equation 2 above, δx and δu denote any measurement errors based on flight measurement data from the flight measurement block **206** (the flight measurement data indicated as δ and χ in FIG. **3**). In particular, sources of measurement error from the flight measurement block **206** include sensor noise and sensor bias. Additional sources of measurement error include, without limitation, sensor drift, sensor dynamics, and sensor time delay. From the control surface positions and actual aircraft states provided by the flight measurement block **206**, an estimated angular acceleration of the aircraft **104** is calculated in the aircraft model block **314** as illustrated below in Equation 3.

$$\begin{aligned}\hat{\dot{\omega}} &= C\hat{f}(x^m, u^m) \\ &= -J^{-1}\omega^m \times J\omega^m + \\ &\quad J^{-1}[\tau_{prop}(x^m, u^m) + \tau_{aero}(x^m, u^m)]\end{aligned} \qquad \text{(Equation 3)}$$

With respect to Equation 3 above, J represents an estimate of the inertia matrix, τ_{prop} represents an estimate of the moments generated by the propulsion system of the aircraft **104** about the center-of-gravity of the aircraft **104**, and τ_{aero} represents an estimate of the aerodynamic moments about the center-of-gravity of the aircraft **104**. In the example embodiment of FIG. **3**, a value for measured angular acceleration $\dot{\omega}^m$ results from differentiating $\omega^m=Cx^m$ as illustrated below in Equation 4.

$$\begin{aligned}\dot{\omega}^m &= \frac{d(Cx^m)}{dt} \\ &= \frac{d(Cx + C\delta x)}{dt} \\ &= \dot{\omega} + \delta\dot{\omega}\end{aligned} \qquad \text{(Equation 4)}$$

With respect to Equation 4 above, $\delta\dot{\omega}$ represents sensor noise. Taking the difference of the measured angular acceleration of the aircraft **104** with the actual angular acceleration of the aircraft **104** results in the error signal e, as illustrated below in Equation 5.

$$\begin{aligned}e &= \hat{\dot{\omega}} - \dot{\omega}^m \\ &= \hat{\dot{\omega}} - \dot{\omega} - \delta\dot{\omega} \\ &= C\hat{f}(x+\delta x + \delta u) - Cf(x, u) - \delta\dot{\omega}\end{aligned} \qquad \text{(Equation 5)}$$

Subsequently, (x_0, u_0) of Equation 5 is considered a trim condition of the aircraft **104** (that is, $f(x_0, u_0)=0$). Taking the Taylor series expansion of e about (x_0, u_0) and keeping only first order terms results in the expression illustrated below with respect to Equation 6.

$$e \approx \underbrace{C\hat{f}(x_0+\delta x, u_0+\delta u) - \delta\dot{\omega}}_{\text{trim and measurement errors}} + \underbrace{C\Delta A\Delta x + C\Delta B\Delta u}_{\text{model mismatch}} \qquad \text{(Equation 6)}$$

With respect to Equation 6 above, $\Delta x=x-x_0$, $\Delta u=u-u_0$,

$$\Delta A = \left.\frac{\partial\hat{f}(x+\delta x, u+\delta u)}{\partial x}\right|_{trim} - \left.\frac{\partial f(x,u)}{\partial x}\right|_{trim},$$

and

$$\Delta B = \left.\frac{\partial\hat{f}(x+\delta x, u+\delta u)}{\partial u}\right|_{trim} - \left.\frac{\partial f(x,u)}{\partial u}\right|_{trim}$$

The residual band pass filter **304** combines each error signal e_1 to e_3 (once filtered) in the residual signal multiplexer **324** to create the residual signal **332**. The low pass filter function **320** removes one or more errors due to sensor noise and high-frequency un-modeled sensor dynamics (for example, aircraft flexure of the aircraft **104**) in all three axes of motion. The high pass filter function **322** removes control surface trim and sensor bias errors in all three axes of motion.

Fault Detection Error Threshold

The threshold signal **330** is the tightly bound upper limit of the one or more potential differences between the at least three reference commands r_1 to r_3 and the at least three error signals e_1 to e_3. When the comparator function **328** determines the residual signal **332** is greater than or equal to the threshold signal **330**, the fault signal **334** indicates that a fault has been detected. In one implementation, the fault signal **334** equals one when the fault is detected. When the fault signal **334** is equal to one, the fault detection module **300** (the fault detection block **210**) informs the fault isolation block **209** of FIG. **2** to estimate a change in H^M (ΔM^M) as discussed above with respect to FIG. **2**. When the aircraft **104** of FIG. **1** does not experience any faults, the residual signal **332** is less than the threshold signal **330**.

For each reference command r received from the flight command block **204** of FIG. **2**, an upper bound is derived in the threshold function **302**. The upper bound limits a modeling mismatch between estimated (that is, predictions made by the one or more reference commands r) and the non-faulted, actual aircraft states (for example, angular acceleration) from the aircraft model block **314**. The threshold function **302** tightly bounds the size of the modeling mismatch in order to minimize the number of false alarms (that is, flagging a fault that has not occurred) and the number of missed detections (that is, not flagging a fault when one has occurred).

The threshold function **302** represents an upper bound of a linear time-invariant transfer matrix G(s) of the at least three reference commands r_1 to r_3 to the residual signal **332**. An impulse response of G(s) is denoted by g(t), and $g_i(t)$ denotes an i^{th} row of G(s). An i^{th} element of $\tilde{e}$ is illustrated below in Equation 7.

$$\tilde{e}_i(t) = \int_0^t g_i(\tau) r(t-\tau)\, d\tau \quad \text{(Equation 7)}$$

An upper bound for $|\tilde{e}_i(t)|$ is derived as illustrated below in Equation 8.

$$\text{(Equation 8)}$$

$$|\tilde{e}_i(t)| = \left| \int_0^t g_i(\tau) r(t-\tau)\, d\tau \right| \le \int_0^t |g_i(\tau) r(t-\tau)|\, d\tau \le \int_0^t \sum_{j=1}^{3} |g_{ij}(\tau) r_j(t-\tau)|\, d\tau \begin{pmatrix} \text{equal to } |\tilde{e}_i(t)| \text{ when} \\ r_j(t-\tau) = \operatorname{sgn}[g_{ij}^{*}(\tau)],\ \forall\, \tau \le t \end{pmatrix} \begin{pmatrix} \text{choose } F_{ij}(s) \text{ with } \sum_{j=1}^{3} |g_{ij}(\tau)| \\ |r_j(t-\tau)| \le \sum_{j=1}^{3} f_{ij}(\tau) |r_j(t-\tau)|,\ \forall\, \tau \le t \end{pmatrix} \le \underbrace{\int_0^t f_{ij}(\tau) |r_j(t-\tau)|\, d\tau}_{\text{The threshold function 302 for } \tilde{e}_i(t)}$$

With respect to Equation 8 above, the threshold function **302** for $\tilde{e}_i(t)$ is graphically depicted in FIG. **3** as the absolute measurement functions **306**$_1$ to **306**$_3$, the threshold filter functions **308**$_1$ to **308**$_3$, and the threshold signal multiplexer **326**. The threshold filter functions **308**$_1$ to **308**$_3$ (represented as first-order filters $F_{ii}(s)$ in Equation 9 below) tightly bounds $|\tilde{e}_i(t)|$. A mathematical model of the first-order filters $F_{ii}(s)$ is illustrated below with respect to Equation 9.

$$F_{ii}(s) = \frac{k_i}{T_i s + 1}, \text{ with } k_i,\ T_i \in R \quad \text{(Equation 9)}$$

Tunable Aircraft Fault Detection

In one implementation, to achieve a particular balance between modeling uncertainty and the number of missed detections, $T_i = 2$ seconds for all three axes with respect to Equation 9 above. The selection of filter gains k_i (for the first-order filters F_{ii}), along with a suitable model of sensor bias from each of the bias model blocks **310**, generates a fault detection classifier for each of the threshold filter functions **308**$_1$ to **308**$_3$. The fault detection classifier separates faulted flight data from non-faulted flight data for each axis of motion. The classification of faulted vs. non-faulted flight data results in a tunable threshold function **302**.

In the example embodiment of FIG. **3**, each of the threshold filter functions **308**$_1$ to **308**$_3$ classify every flight command dataset (from the at least three reference commands r_1 to r_3) using Statistical Learning Theory (SLT). Alternate classification methods are possible. SLT allows the threshold function **302** to learn a classifier function y =f(x) that will correctly classify unseen fault examples (that is, fault samples) as an expected risk. The expected risk measures performance of a candidate solution f as illustrated below in Equation 10.

$$R[f] = \int L(f(x), y)\, dP(x,y) \quad \text{(Equation 10)}$$

With respect to Equation 10 above, R is the risk functional ranging over
[0, 1], P(x, y) represents a probability density function (PDF) of the filter gains k_i of the threshold filter functions **308** (x) and the sensor bias from the bias model blocks **310** (y), and L is the loss function defined as illustrated below with respect to Equation 11.

$$L(f(x), y) = \begin{cases} 0 & \text{if } f(x) = y \\ 1 & \text{if } f(x) \ne y \end{cases} \quad \text{(Equation 11)}$$

Along with calculating the expected risk, a risk over each of the flight command datasets, or an empirical risk, is determined as illustrated below in Equation 12.

$$R_{emp}[f] = \frac{1}{N} \sum_{i=1}^{N} L(f(x_i), y_i) \quad \text{(Equation 12)}$$

In one implementation, an empirical risk minimization (ERM) controls complexity (that is, capacity) of the function f of Equation 12 above. In one implementation, the classifier function uses a Vapnik-Chervonenkis (VC) dimension to measure complexity. The VC dimension of the classifier f measures the largest number of examples which can be modeled by a family of f. The VC dimension of the function f bounds the expected risk of Equation 10 as a function of the empirical risk of Equation 12 and a number of available examples. Moreover, a probability $(1-\eta)$ illustrates that the expected risk $R[f]$ of classification by the function f is upper-bounded by the sum of the empirical risk $R_{emp}[f]$ and a VC confidence function as illustrated in Equation 13 below.

$$R[f] \le R_{emp}[f] + \left[\frac{h\left(\log\left(\frac{2N}{h}\right) + 1\right) - \log\left(\frac{\eta}{4}\right)}{N} \right]^{\frac{1}{2}} \quad \text{(Equation 13)}$$

With respect to Equation 13, h is the VC dimension of f, N is the number of examples, and a second term on the right-hand side is the VC confidence function. To reduce the expected risk in classification, the classifier minimizes both the empirical risk and the VC confidence using Structural Risk Minimization (SRM). As the N/h term grows larger, the VC confidence term becomes smaller and the expected risk becomes closer to the empirical risk. For a fixed size of the dataset, the expected risk is reduced by reducing the VC dimension of the classifier.

The bound on the expected risk is used to estimate a sample size within a prescribed confidence level (that is, the sample size guarantees a desired degree of confidence in the classification results obtained by f). To estimate the sample size, ϵ

represents an error tolerance between the estimated and empirical risks as illustrated below in Equation 14.

$$P(\sup(R[f]-R_{emp}[f])<\epsilon)>1-\eta \quad \text{(Equation 14)}$$

With respect to Equation 14 above, any classification based on f is (with a confidence of $(1-\eta)$) correct within a tolerance of ϵ. Equation 15 is derived below based on Equations 13 and 14 above.

$$\epsilon < \left[\frac{h\left(\log\left(\frac{2N}{h}\right)+1\right)-\log\left(\frac{\eta}{4}\right)}{N}\right]^{\frac{1}{2}} \quad \text{(Equation 15)}$$

With the values of η, ϵ and h, the threshold function **302** computes the size of each of the flight command datasets (represented as N) using Equation 15. In the example embodiment of FIG. **3**, one or more values are used for ϵ and η (for example, of the order of 0.01-0.10). Moreover, using ϵ=0.1, η=0.01, and h=3 (a VC dimension for a 2-D hyperplane classifier), Equation 15 computes the lower bound on N as approximately 3200. Tighter bounds for values of ϵ and η reduce N by a substantial order of magnitude. In one implementation, N (that is, the flight command dataset) is reduced by a factor of 18.

In one implementation, a separating hyperplane substantially maximizes a margin (that is, the distance between the decision surface and the nearest data-point of each class) for the (linearly-separable) dataset from the viewpoint of SRM. A VC dimension of the separating hyperplane h with margin m bounded is illustrated below in Equation 16.

$$h \le \min\left(\frac{R^2}{m^2}, n\right)+1 \quad \text{(Equation 16)}$$

With respect to Equation 16 above, n is the dimensionality of the input space, and R is the radius of the smallest hypersphere containing all the input vectors. The fault detection module **300** substantially maximizes the margin m to substantially minimize the VC dimension of the separating hyperplane. In one implementation, the separating hyperplane has substantially no empirical error (that is, the separating hyperplane correctly separates the dataset). By correctly separating each flight command dataset into faulted and non-faulted responses, the margin is substantially maximized and the upper bound on the expected risk is substantially minimized (that is, the fault detection classifier provides a statistical guarantee that the threshold function **302** will correctly identify faulted and non-faulted flight data).

In one implementation, in order to correctly separate the reference command dataset, the separating hyperplane involves separating a set of training vectors belonging to two separate classes as illustrated below in Equation 17, with a hyperplane as illustrated below in Equation 18.

$$D=\{(x_1, y_1), (x_2, y_2), \ldots, (x_N, y_N)\}, x\in R^n, y\in\{-1,1\} \quad \text{(Equation 17)}$$

$$\langle w,x\rangle+b=0 \quad \text{(Equation 18)}$$

In one implementation, the fault detection module **300** includes a canonical hyperplane where the parameters w (representing the filter gains k_i of the threshold functions **308**) and b (representing the sensor bias of the bias model blocks **310**) are constrained as illustrated below in Equation 19.

$$\min_i|\langle w,x\rangle+b|=1 \quad \text{(Equation 19)}$$

An optimal separating hyperplane must satisfy the following constraints as illustrated below in Equation 20, with a margin given as illustrated in Equation 21.

$$y_i[\langle w, x_i\rangle + b] \ge 1,\ i \in \{1, 2, \ldots, N\} \quad \text{(Equation 20)}$$

$$\begin{aligned}\rho(w, b) &= \min_{x_i:y_i=-1}\frac{|\langle w, x_i\rangle + b|}{\|w\|} + \min_{x_i:y_i=-1}\frac{|\langle w, x_i\rangle + b|}{\|w\|} \\ &= \frac{1}{\|w\|}\left[\min_{x_i:y_i=-1}|\langle w, x_i\rangle + b| + \min_{x_i:y_i=-1}|\langle w, x_i\rangle + b|\right] \\ &= \frac{2}{\|w\|}\end{aligned} \quad \text{(Equation 21)}$$

Optimizing the dataset of each of the threshold filter functions $\mathbf{308}_1$ to $\mathbf{308}_3$ is illustrated below in Equations 22 and 23.

$$\max_{\alpha}\min_{w,b}\Phi(w, b, \alpha),\ \text{where} \quad \text{(Equation 22)}$$

$$\Phi(w, b, \alpha) = \frac{1}{2}\|w\|^2 - \sum_{i=1}^{N}\alpha_i(y_i[\langle w, x_i\rangle + b] - 1 \quad \text{(Equation 23)}$$

With respect to Equation 23 above, α_i are Lagrangian multipliers with $\alpha_i \geqq 0$. Casting Equation 23 as a quadratic programming (QP) problem using a dual formulation is illustrated below in Equation 24.

$$w^* = \sum_{i=1}^{N}\alpha_i y_i x_i \qquad b^* = -\frac{1}{2}\langle w^* x^r + x^s\rangle \quad \text{(Equation 24)}$$

In one implementation, and with respect to Equation 24 above, x^r represents a support vector from each class (that is, fault and non-fault data) of the flight command dataset, and x^s represents a support vector from each class of the sensor bias readings that both satisfy Equation 25 as illustrated below.

$$\alpha^r, \alpha^s>0,\ y^r=-1,\ y^r=1 \quad \text{(Equation 25)}$$

With respect to Equation 25 above, a classifier function for the support vectors x^r and x^s is illustrated below in Equation 26.

$$f(x)=sgn(\langle w^*,x\rangle+b^*) \quad \text{(Equation 26)}$$

With respect to Equation 26 above, w*(a vector of size 3) represents the optimal gains k_i for each of the threshold filter functions $\mathbf{308}_1$ to $\mathbf{308}_3$, and b*(a vector of size 3) represents the optimal bias for each of the bias model blocks $\mathbf{310}_1$ to $\mathbf{310}_3$. The support vectors x^r and x^s classify the faulted and non-faulted flight command data in each of the threshold filter functions $\mathbf{308}_1$ to $\mathbf{308}_3$. The fault detection classifier trains (that is, tunes) the threshold function **302** to optimally classify the faulted and non-faulted flight data and ignore the non-faulted data.

While the methods and techniques described here have been described in the context of a fully-functioning simulated aircraft fault detection system, apparatus embodying these techniques are capable of being distributed in the form of a computer readable medium of instructions and a variety of forms that apply equally regardless of the particular type of signal bearing media actually used to carry out the distribution. Examples of computer readable media include recordable-type media, such as a portable memory device, a hard disk drive, a RAM, CD-ROMs, DVD-ROMs; and transmission-type media, such as digital and analog communications links, wired or wireless communications links using transmission forms such as, for example, radio frequency and light wave transmissions. The computer readable media may take the form of coded formats that are decoded for actual use in an aircraft flight system, including flight system **100** of FIG. **1**.

What is claimed is:

1. A method for detecting faults in an aircraft, the method comprising:
in a programmable processor:
predicting at least one state of the aircraft;
processing corresponding actual, non-faulted aircraft state and a faulty aircraft state to at least one bias value and at one threshold filter function;
generating at least one threshold value based on a first reference command signal;
tuning the at least one threshold value to upper bound the size of a mismatch between the at least one predicted state and the corresponding actual state based on the at least one bias value and the at least one threshold filter function; and
if the mismatch between the at least one predicted state and the corresponding actual state is greater than or equal to the at least one threshold value, indicating that at least one fault has been detected.

2. The method of claim **1**, wherein predicting the at least one state further comprises estimating angular acceleration of the aircraft.

3. The method of claim **1**, further comprising classifying the faulted flight data from the non-faulted flight data for each axis of motion.

4. The method of claim **3**, wherein the at least one threshold filter function and the at least one bias value statistically guarantee the classification of the faulted and non-faulted flight data within a prescribed confidence level.

5. The method of claim **1**, wherein indicating that the at least one fault has been detected further comprises notifying a display on a flight deck of the aircraft upon successful detection of the at least one fault.

6. The method of claim **1**, wherein tuning the at least one threshold value to upper bound the size of a mismatch further comprises:
filtering an absolute value of the first reference command signal with the at least one threshold filter function to generate a filtered reference command signal; and
adding the at least one bias value to the filtered reference command signal.

7. The method of claim **1**, wherein the at least one threshold filter function comprises a filter gain.

8. A method for detecting faults in an aircraft, the method comprising:
in a programmable processor:
predicting at least one aircraft state based on responses from flight measurement data;
calculating a difference between the predicted aircraft state and a corresponding measured state of the aircraft;
processing a corresponding actual, non-faulted aircraft state and a faulty aircraft state to calculate at least one filter gain and at least one bias value;
determining a threshold of an upper bound for the difference between the predicted aircraft state and the corresponding measured state based on the at least one bias value and the at least one filter gain;
comparing the threshold with the difference between the predicted aircraft state and the corresponding measured state; and
if the difference is greater than or equal to the threshold, indicating that at least one fault has been detected.

9. The method of claim **8**, wherein predicting the at least one aircraft state comprises estimating operational behavior of the aircraft in a non-fault state in response to one or more reference commands.

10. The method of claim **8**, wherein calculating the difference further comprises deriving the corresponding measured state from actual flight measurement data.

11. The method of claim **8**, wherein determining the threshold further comprises:
classifying faulted and non-faulted flight measurement data; and
ignoring the non-faulted flight measurement data.

12. The method of claim **11**, further comprising calculating the at least one filter gain and the at least one bias value that statistically guarantees the classification of the faulted and non-faulted flight measurement data within a prescribed confidence level.

13. The method of claim **8**, wherein indicating further comprises notifying a flight deck control display with a status and potential impact of the at least one detected fault on the aircraft.

14. The method of claim **8**, wherein determining the threshold further comprises wherein the threshold is based on a first reference command signal.

15. The method of claim **14**, wherein determining the threshold further comprises filtering an absolute value of the first reference command signal with the at least one filter gain and adding the at least one bias value.

16. A method for detecting a fault in an aircraft, comprising:
in a programmable processor:
generating a threshold signal based on at least one bias value added to a reference command signal filtered by at least one threshold filter function;
generating a residual signal based on a band passed filtered error function, wherein the band passed filtered error function is based on the difference between a measured state of the aircraft and a corresponding estimated state;
comparing the threshold signal and the residual signal;
tuning the threshold signal based on processing a corresponding actual, non-faulted aircraft state and a faulted aircraft state to compute the at least one bias value and at least one threshold filter function; and
indicating that at least one fault is detected when the residual signal is equal to or greater than the threshold signal.

17. The method of claim **16**, wherein tuning the threshold signal further comprises classifying faulted flight data from non-faulted flight data for each axis of motion.

18. The method of claim **17**, wherein classifying faulted flight data from non-faulted flight data for each axis of motion further comprises calculating at least one threshold filter function and at least one bias value that statistically guarantees the classification of the faulted and non-faulted flight data within a prescribed confidence level.

19. The method of claim **16**, wherein indicating further comprises displaying a notification on a flight deck of the aircraft.

* * * * *